Pol. J. Environ. Stud. Vol. 30, No. 3 (2021), 2301-2312
DOI: *10.15244/pjoes/125851* ONLINE PUBLICATION DATE: 2021-01-28

Original Research

Tobacco Stalk Waste Biomass Holds Multilayer and Spontaneous Adsorption Capabilities for Reactive Black 5 Dye: Equilibrium Modelling and Error Function Analysis

Jehanzeb Ali Shah[1], Cyrus Raza Mirza[2], Tayyab Ashfaq Butt[2], Walid M.A. Khalifa[2], Hatem H. Gasmi[2], Hajira Haroon[1,5], Muhammad Saqib Khan[1], Muhammad Arif Ali[3], Iftikhar Zeb[4], Sajid Hussain Shah[1], Bilal Ahmad Zafar Amin[6], Muhammad Bilal[1]*

[1]Department of Environmental Sciences, COMSATS University Islamabad, Abbottabad Campus, 22060, Abbottabad, Pakistan
[2]Department of Civil Engineering, University of Hail, Hail Province, 55476, Saudi Arabia
[3]Department of Soil Science, Bahauddin Zakariya University, Multan, 60800, Punjab, Pakistan
[4]Department of Biotechnology, COMSATS University Islamabad, Abbottabad Campus, 22060, Abbottabad, Pakistan
[5]Department of Environmental Sciences, University of Haripur, 22620, KP, Pakistan
[6]Energy Research Centre (ERC) COMSATS University Islamabad, Lahore Campus, 54000, Lahore

Received: 27 February 2020
Accepted: 29 July 2020

Abstract

Tobacco stalk biomass (TSB) is explored for reactive black 5 (RB5) dye treatment in batch reactor. TSB displayed RB5 adsorption efficiency of 93.5% at 120 min. The RB5 data were fitted to linear and non-linear isotherms and kinetic models. Error functions were determined to have a holistic view on optimum parameters and to validate prediction of models. Harkin-Jura exhibited better fit than that of Freundlich and Langmuir isotherms suggesting multilayer adsorption of RB5 onto TSB on the basis of R^2 and chi-square (χ^2) error values. Adsorption kinetics was best explained by intraparticle diffusion model (IPD) at increasing initial concentration of RB5. Among the error functions evaluated, the χ^2 values for the IPD model were found to be smaller than those for PSO. This suggests that kinetics of RB5 dye is better controlled by IPD phenomenon. Fourier transform infrared spectroscopy confirms the physical adherence of dye to the adsorbent. Values of Gibbs free energy were found to be -19.55 -21.41, -23.40 and -25.33 kJ/mol which shows spontaneous adsorption. Moreover, it is found that TSB adsorbent could be utilized as the effective and economically viable adsorbent for RB5 dye from aqueous solution.

Keywords: tobacco biomass, spontaneous adsorption, RB5 dye, multilayer, error function analysis, isotherm, kinetic model

*e-mail: malikmohammadbilal@gmail.com
mbilal@cuiatd.edu.pk

Introduction

Tobacco is one of the major non-edible cash crop around the globe. In Pakistan, it is reported that total area under tobacco cultivation is 46332 hectare, with 106.78 M Kg of production (different types of leaves). This sector contributed a worth of 25.74 M USD on export of 7.30 M Kg for the year 2017-2018. Thus the possible fate tobacco stalks (produced in huge amount) includes: (i) chopped in fields for microbial turnover; (ii) left in fields; (iii) used as fuel for cooking at household level. Tobacco stalks are rich source of nicotine, therefore, may cause health issues and environmental problems if the particular soil blown away in nearby cities or populated towns in the vicinity. So this lignocellulosic waste source can be given a high environmental value if used for the removal of textile hazardous dyes from the waste streams [1].

Synthetics colorants are widely synthesized and applied in textile industry. Estimates demonstrate more than 100,000 dyes in the market with estimated production of 700,000 tons per annum [2]. These dyes are grouped into cationic, anionic, direct and reactive and many others on the basis of structure, mode of action and chemical composition. Lasting impacts and provision of contrasting shades mark the reactive dyes one of the most widely opted and applied group in textile sector. The presence of vinyl sulfone groups increases their water solubility, subsequently this leads towards low fixation ratio and generates densely colored wastewater. These wastewaters impairs photosynthesis and provoke imbalance in delicate food chains and presence of azo bonds in dyes lead the production of carcinogenic amino groups on degradation, thus, pose threats to all the aquatic organisms [3]. Reactive black 5 (RB5) is one of the most commonly used dyes in textile industry. The azo group, acting as chromophore, covalently bonds with cellulose of substrate. However, significant hydrolysis yields highly colored water [4]. The unique characteristics of this dye, e.g., resistance towards biodegradation and persistence, make it really difficult to adopt biological and other treatment methods.

The adsorption process seems to be a robust option due to ease of operation, low cost, simplicity and higher efficiency [5]. Agriculture based lignocellulosic biomasses have been used to treat dyes loaded wastewater, for instance, sun flower seed hulls [6], corncob and corn silk [7, 8], wheat bran [9], almond shell residue [10], golden shower pod, coconut shell, and orange peel [11] and date palm stones [12]. The presence of biopolymers such cellulose, hemicellulose, lignin, polysaccharides rank these natural biomasses as active choice for the removal of dyes from wastewaters. As they are renewable resources and contain oxygen containing functional groups which could play major role for the removal water soluble reactive dyes from aqueous phase. This investigation aims to explore the potential of tobacco stalks biomass (TSB) as an adsorbent for the separation of reactive black 5 (RB5), an azo dye, from aqueous solution. The adsorption behavior was studied using isotherm and kinetic models. Error analysis was carried out to determin the goodness of fit for isotherm and kinetic models.

Materials and Methods

Chemicals and Dye Solution

Reactive black 5, anionic dye (CAS Number 17095-24-8, Molecular formula $C_{26}H_{21}N_5Na_4O_{19}S_6$, molecular weight 991.82 g/mol and λ_{max} = 598 nm) was purchased from Sigma Aldrich and was used without further purification. All chemicals used were of analytical grade. Stock solutions were freshly prepared with deionized water for every experiment in order to obtain coherent and reliable results. Subsequent dilutions were made when required. pH adjustments were performed using 0.1 M HCl and 0.1 M NaOH solutions.

Adsorbent Preparation

Tobacco stalks biomass (TSB) was collected from local agricultural fields, situated in district Mansehra, Khyber Pakhtunkhwa, Pakistan. These stalks were firstly washed multiple times with distilled water in order to remove adhered dirt and other impurities. Cleaned biomass was then placed in drying oven at 60ºC for 24 h until constant weight of biomass was obtained. Afterward dried stalks were ground to fine powder. This powder was placed in an air tight container for onward usage.

Fourier Transform Infrared Spectroscopy (FTIR)

The diverse functional groups on the surface of adsorbent play a pivotal role in the adsorption of pollutants from waste streams. Analytical grade 200 mg of KBr in powdered form was thoroughly mixed with 2 mg of TSB followed by drying in order to eradicate the moisture. Two FTIR spectrums were recorded for TSB with and without RB5 loading in the spectral range of 600 to 4000/cm using Spectrum 1000, Bruker, Germany.

Scanning Electron Microscopy (SEM) and Energy Dispersive X-ray (EDX) Analyses

In order to better understand the surface characteristics of the adsorbent, scanning electron microscopy was performed using Hitachi Japan, S-3000N. TSB adsorbent was analyzed in acceleration voltage range of 5-20 kV and constant distance of 25 mm was maintained between pole and sample. Elemental composition of TSB was determined through EDX analysis.

Point of Zero Charge (pHpzc) Determination

pH_{pzc} for TSB adsorbent was determined by contacting 50 mL of 0.01 M sodium chloride (NaCl) solution with 3 g/L adsorbent under variable pH range from 2 to 12 and contact time of 72 h was maintained. The pH adjustments were performed using 0.1 M HCl and 0.1 M NaOH solutions. The change in ΔpH (initial pH-final pH) was plotted against initial pH and point of intersection was marked as pH_{pzc} and/or the point of adsorbent neutrality.

Batch Adsorption Experiment

Batch experimental work was performed in 50 mL Erlenmeyer flasks containing 20 mL of RB5 dye solution, TSB adsorbent dosage (0.4-2 g/L), initial dye concentration (10-210 mg/L), pH (1-7), temperature (30-60ºC) and contact time (0-240 min). The suspension obtained after filtration was analyzed at λ_{max} = 598 nm using double beam T80^{+} UV-VIS spectrophotometer. Adsorption capacity (mg/g) and removal (%) of RB5 by TSB were calculated using Equations 1, 2 and 3 respectively.

$$Removal\ (\%) = \left(\frac{C_0 - C_f}{C_0}\right) 100 \quad (1)$$

$$q_t = \left(\frac{C_0 - C_t}{m}\right) V \quad (2)$$

$$q_e = \left(\frac{C_0 - C_e}{m}\right) V \quad (3)$$

...where q_e and q_t denote the adsorption capacity (mg/g) at equilibrium and any time *t* respectively. C_0, C_f, C_e, C_t, V and m indicate the initial adsorbate concentration (mg/L), final adsorbate concentration (mg/L), residual adsorbate concentration (mg/L) at equilibrium, at time *t*, volume of aqueous solution (L) and mass of adsorbent (g/L) respectively.

Desorption Studies

Regeneration of the adsorbent is a key performance parameter, which is considered as an eco-friendly solution to mimic the problem of water pollution and to better understand the reusability of adsorbent and mechanism of adsorption. In this study, initially 1 g/L of TSB adsorbent was contacted with 80 mg/L of initial RB5 dye concentration at agitation speed of 30 rpm, 30ºC temperature and contact time of 2 h. For desorption study, RB5 loaded adsorbent was subjected to a range of eluents ranging from simple distilled water at 40 and 50°C to variable molar strengths of 0.25, 0.5, 0.75 and 1 M NaOH. Rest of batch conditions were kept same as mentioned above. The RB5 dye desorption was calculated using Equation 4.

$$Desorption\ (\%) = \left(\frac{q_{ads}}{q_{bd}}\right) 100 \quad (4)$$

...where q_{ads} and q_{bd} refer to the amount of adsorbate concentration (mg/L) adsorbed to and desorbed from TSB adsorbent respectively.

Kinetics, Isotherms and Thermodynamic Studies

For kinetic study, different initial RB5 dye solutions (20-80 mg/L) were agitated for predetermined time intervals from 10 to 120 min. For isotherm study, dye containing aqueous solutions having different concentration were agitated until established equilibrium time. For thermodynamic study, batch experiments were executed at variable temperatures of 303.15, 313.15, 323.15 and 333.15 K, keeping the equilibrium time, adsorbent dose of 1 g/L, agitation of 150 rpm, 30 mg/L of RB5 dye concentration and pH 2.

Error Function Analysis and Best Fit Models

The data transformations can modify the error structure during the linearization of isotherm equation, therefore, may violate the normality assumptions and error variance. Reports explained the deviation between q_{exp} and q_{cal} in linear form of isotherm curves on the basis of coefficient of determination (R^2), however, this does not explain the errors in non-linear form of isotherm equations. Therefore, it is essential to determine the error functions to validate the goodness of fit for both linear and non-linear isotherm models. To accomplish this task, the linear and non-linear isotherm data were computed to different error functions to have a holistic view on the optimum parameters and prediction of isotherms. The error distribution between experimental and model predicted values of adsorption capacities were minimized by reducing respective error functions using solver add-in Microsoft® excel 2013 and no constraints were applied during this minimization technique and optimization of model constants. Small errors serves the basis to claim good curve fitting.

Among the studied error functions (Equations 5-14), coefficient of determination (R^2) between experimental and predicted adsorption capacities of TSB for RB5 was determine to explain the variance about the mean for non-linear regression [13]. Chi-square (χ^2) has been widely applied to determine the goodness of fit between the experimental $q_{e\ exp}$ (mg/g) with those predicted $q_{e\ cal}$ (mg/g) by model [14]. This function express the each squared difference divided by the corresponding $q_{e\ cal}$ value. This shows that more close the qe cal to qe exp, less the χ^2 and vice versa. Therefore, this function can provide a good measurement scale to weigh the fit and identify the best fit isotherm. Average relative error (ARE) minimizes fractional error distribution across the entire concentration range and reveal the susceptibility to underestimate or overestimate the

experimental data value [15]. Standard deviation of relative errors (S_{RE}) is a measure of how tightly packed the data is around the mean and Marquardt's percent standard deviation (MPSD) error function is similar to geometric mean error distribution which was modified to allow for number of degrees of freedom in the system [16]. Normalized standard deviation (NSD, Δq (%)) error function indicate the closeness of model value to that $q_{e\,exp}$ [16], therefore, lower the value of Δq (%) higher the goodness of model fit and vice versa. Additionally, smaller the RMSE value, better the curve fitting. EABS method is similar to ERRSE, however, this function introduce a biasness in the curve fitting towards high concentration range [16]. Root mean square error (RMSE) is also called as root mean square deviation [17], which sums the error's magnitude and is extensively used error function to a good estimate of accuracy Hybrid functional error (HYBRID) [17] was developed initially to enhance the better fit to ERRSQ at lower concentration range by diving the ERRSQ with adsorption capacity and adding the degree of freedom into the divisible, i.e., number of data points minus the number of parameters in the equation.

Coefficient of determination (R^2)

$$= \frac{\Sigma\left(q_{t_{cal}} - \bar{q}_{t_{exp}}\right)^2}{\Sigma\left(q_{t_{cal}} - \bar{q}_{t_{exp}}\right)^2 + \Sigma\left(q_{t_{cal}} - q_{t_{exp}}\right)^2} \quad (5)$$

Nonlinear chi-square test (χ^2)

$$= \sum_{i=1}^{n} \frac{\left(q_{e\,exp} - q_{e\,cal}\right)^2}{q_{e\,cal}} \quad (6)$$

Average relative error (ARE)

$$= \frac{1}{n} \sum_{i=1}^{n} \left(\frac{q_{e\,exp} - q_{e\,cal}}{q_{e\,exp}} \right) \quad (7)$$

Standard deviation of relative errors (S_{RE})

$$= \sqrt{\sum_{i=1}^{n} \frac{\left[\left(q_{e,exp} - q_{e\,cal}\right) - ARE\right]^2}{n-1}} \quad (8)$$

Normalized standard deviation (NSD)

$$= 100 \sqrt{\frac{1}{n-1} \sum_{i=1}^{n} \left(\frac{q_{e\,exp} - q_{e\,cal}}{q_{e\,exp}} \right)^2} \quad (9)$$

Residual root mean square error (RMSE)

$$= \sqrt{\frac{1}{n-2} \sum_{i=n}^{n} \left(q_{e\,exp} - q_{e\,cal}\right)^2} \quad (10)$$

Marquardt's percent standard deviation (MPSD)

$$= 100 \sqrt{\frac{1}{n-p} \sum_{i=1}^{n} \left(\frac{q_{e\,exp} - q_{e\,cal}}{q_{e\,exp}} \right)^2} \quad (11)$$

Sum of absolute error (EABS)

$$= \sum_{i=1}^{n} \left| q_{e,exp} - q_{e,cal} \right| \quad (12)$$

Hybrid functional error (HYBRID)

$$= \frac{100}{n-p} \sum_{i=1}^{n} \frac{\left(q_{e\,exp} - q_{e\,cal}\right)^2}{q_{e\,exp}} \quad (13)$$

Sum of Square of the error (ERRSQ)

$$= \sum_{i=1}^{n} \left(q_{e\,exp} - q_{e\,cal}\right)^2 \quad (14)$$

Results and Discussion

FTIR Analysis

The detailed FTIR analysis of raw and RB5 loaded TSB is shown in Fig. 1. The characteristic peaks at 3318/cm and 2932/cm were assigned to the $-NH_2$ group and C-H stretching [18]. Likewise spectral peak recorded at 1617/cm confirms the presence of H_2O mode type bending [19]. The aromatic C-N stretching and ester bonding were observed, respectively, at 1329/cm and 1242/cm [20]. Two peaks documented at 1025/cm and 893/cm exhibited the existence of $-CH_2OH$ (primary hydroxyl group) [21] and deformed OH group [22], respectively. The minimum variability between raw and RB5 treated TSB FTIR spectrum is attributed to the low chemical interaction between anionic dye and functional groups of adsorbent. The changes in intensity also validated the physical adherence of dye molecules to the TSB surface.

SEM and EDX Analyses

Surface morphology of raw and RB5 loaded TSB was explored using SEM and elemental composition of raw TSB was determined by EDX analysis as shown in Fig. 2. It is apparent from the figure that raw TSB contained thick walled pores as well as irregular and elongated structures which could be conducive for the uptake of complex RB5 dye molecules. Dark white spots as well as smoothness in the surface of RB5 loaded TSB revealed the interaction and the conglomeration of

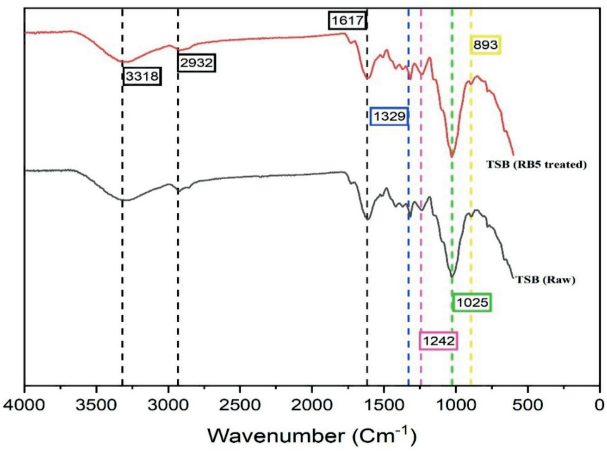

Fig. 1. FTIR Analysis of TSB (Raw) and RB5 (loaded).

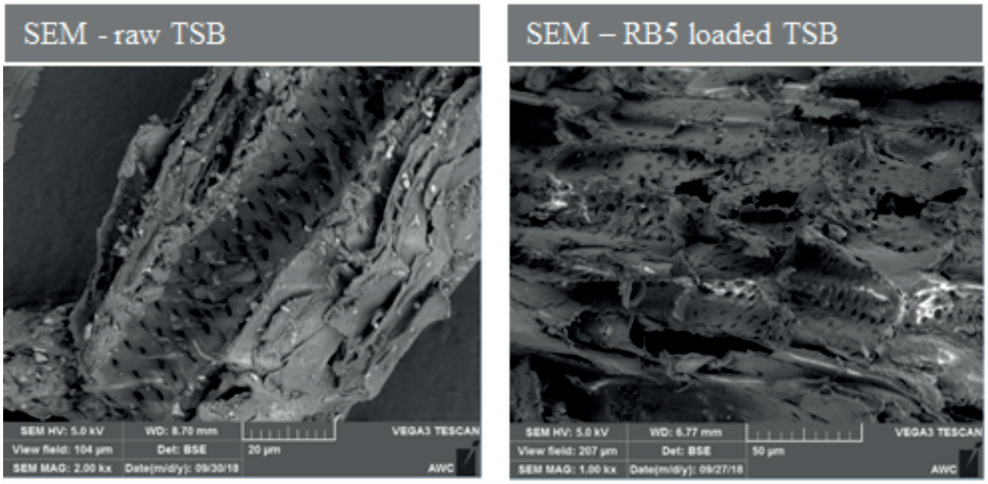

EDX analysis

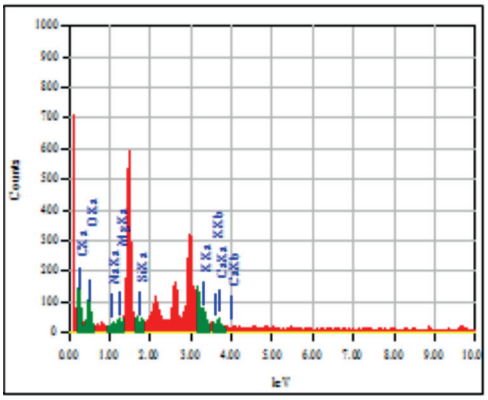

Elements	Mass (%)	Atom (%)
C	23.64	31.95
O	58.06	58.93
Na	1.03	0.73
Mg	5.09	3.40
Si	0.06	0.03
K	5.75	2.39
Ca	6.37	2.58
Total	100	100

Fig. 2. SEM micrographs and EDX analysis of TSB.

dye molecules of RB5 dye molecules onto the surface of TSB adsorbent. EDX exhibited the variable atomic composition of elements in TSB biomass, likewise O (58.93 %), C (31.95 %), Mg (3.40 %), Ca (2.58 %), K (2.39 %), Na (0.73 %) and Si (0.03 %) as it is shown in Fig. 2.

Effect of Contact Time

Equilibrium time is a key parameter in designing and implementing a full-scale adsorption system for treatment of wastewater containing toxic dyes. Fig. 3 describes the adsorption of RB5 dye onto the surface of raw TSB in batch system, keeping 1 g/L TSB, 303 K temperature, agitation speed of 150 rpm and initial concentration of RB5 dye as 30 mg/L. Fig. 3 manifested the initial sharp uptake of RB5 dye by TSB adsorbent (87%, 26.05 mg/g) in first 20 min of contact. This can be correlated with availability of abundant vacant adsorption sites onto the adsorbent surface, therefore, it become easier for for dye molecules to attach either physically through weak Van Der Waal forces or chemically through any kind of bonding either by complexation or ion exchange. Afterwards adsorption process of RB5 onto TSB surface was got slow down and became almost stable (93.28%, 29.78 mg/g) at 120 min. Therefore, all other batch experiments were run for equilibrium time of 120 min.

Initial Concentration of RB5 Dye

The effect of increasing RB5 dye concentration onto TSB capability for dye removal is shown in Fig. 3. RB5 dye removal capability of TSB increased from 9.98 mg/g to 92.84 mg/g which can be associated to probably a high mass-transfer driving force. A similar trend has been observed for reactive dyes adsorption by corn silk [23]. However RB5 adsorption efficiency of TSB decreased from 99.83 to 54.90% with the increasing initial dye concentration from 10 to 190 mg/L. This decline in TSB removal efficiency at high RB5 dye concentrations is related to the fact that nearly all of the active binding areas on the adsorbent surface are filled and number of competing RB5 molecules for the specific active binding sites increased, so dye removal decreased [24].

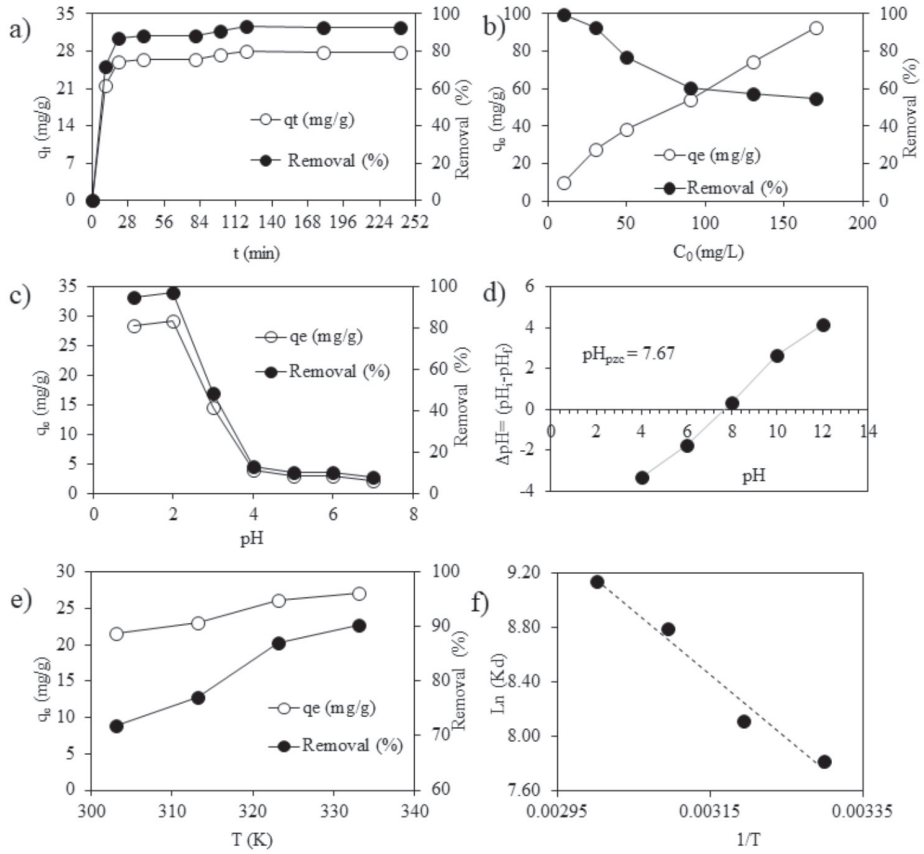

Fig. 3. Effect of process parameters on RB5 dye adsorption by TSB: a) contact time, b) initial dye concentration (c_0), c) pH, d) determination of point of zero charge (pH_{pzc}), e) Temperature, f) Van't Hofs plot.

pH and pHpzc Determination

The alterations in aqueous phase acidity and basicity affect the chemistry of dye groups on one hand and the surface chemistry, availability and dissociation of functional groups present onto the surface of adsorbent on the other. The impact of solution pH on RB5 dye adsorption by TSB was probed in the pH range of 2-7 is shown in Fig. 3 and the the investigation of basic pH range was avoided due to the fact of anionic nature of RB5. It is obvious that RB5 is expressively adsorbed by TSB at lower pH. TSB displayed decreasing adsorption trend of RB5 from 96.97% (29.09 mg/g) to 9.87% (2.96 mg/g) when the solution pH was augmented from 2 to 6 respectively (Fig. 3). The acidic conditions results protonation of the TSB adsorbent surface which is negatively charged due to the presence of slightly anionic cellulose, crafting it appropriate for the holding of anionic reactive dye stuff present in aqueous phase [25]. Similar trends have been reported on reactive dyes adsorption by soybean hull [26], soybean residue [27], alfa fiber powder [28], eucalyptus bark [29], *Trapa bispinosa's* peel and its fruit [30]. pH_{pzc} refers to the situation at which the protonic charge on the surface of adsorbent equals to anionic charge of aqueous solution, resulting in net zero charge on adsorbent's surface. This surface charge becomes negative and positive under the conditions of $pH>pH_{pzc}$ and $pH<pH_{pzc}$ respectively [31]. Therefore, the solution $pH<pH_{pzc}$, the adsorbents surface becomes positively charged due to tendency of high H^+ ions. Thus maximum RB5 dye uptake was observed to be 97% by TSB at pH 2 and this confirms the suitability of TSB adsorbent under the given conditions. Moreover, TSB adsorbent gains negative charge with the increase in initial pH and electrostatic repulsion is developed between adsrbent and anionic RB5 dye due to excess of OH^- ions. As shown in Fig. 3 RB5 dye removal by TSB is reduced.

Temperature and Thermodynamic Studies

Effect of increasing temperature from 303.15 to 333.15 K on RB5 removal efficiency of TSB at equilibirum is shown in Fig. 3. RB5 removal by TSB was enhanced from 71.89 to 90.21% with rising temperature. This exhibits the endothermic nature of adsorption process. This phenomenon can be ascribed to increase in kinetic energy which weakens the bonding forces between dye mlecules, and reduces the swelling effect, therefore, increasing the possiblity of RB5 dye ions to perforate further within TSB adsorbent and thus increase the dye adsorption [32].

The additional RB5 adsorption by TSB with temperature was corroborated by thermodynamic paramters, i.e., changes in Gibbs free energy (*ΔG*), entropy (*ΔS*) and enthalpy (*ΔH*). In order to make equibrium constant (K_d, L/g) dimensionless, K_d was multiplied by solution (water) density (ρw ≈ 1000 g/mL) [33]. The aforesaid thermodynamic parameters were calcuated using slop and intercept of Van't Hoff plot (*lnK_d versus l/T*) as shown in Fig. 3 and following Equations were used:

$$l_n\, K_d(\rho_w) = \frac{q_e}{c_e} \tag{15}$$

$$\ln K_d(\rho_w) = \frac{\Delta S}{R} - \frac{\Delta H}{RT} \tag{16}$$

$$\Delta G = \Delta H - T\Delta S \tag{17}$$

The values of ΔH (38.86 kJ/mol) and ΔS (0.19 kJ/mol) are positive, which verify the endothermic nature and absorption of heat during RB5 and TSB adsorbent interaction. The value of ΔH confirm the physisorption as for chemisorption ΔH is usually less than 40 kJ/mol [34, 35]. Negative ΔG values were found to be -19.55, -21.41, -23.40 and -25.33 kJ/mol, respectively, at 303.15, 313.15, 323.15 and 331.15 K which exhit the suitability and spontaneous adsorption of RB5 dye onto TSB at all temperatures.

Linear and Non-Linear Adsorption Isotherm Fitness Analysis

Isotherm models are applied to investigate the interaction of pollutants with the surface of adsorbent. The fitness of these isotherm models helps in optimizing and determining the favorability of adsorbent. Both the linear and non-linear forms of Harkins-Jura, Freundlich, and Langmuir isotherm models were fitted to RB5 adsorption data and the underlying adsorption behavior was probed. Harkin and Jura model infers a multilayer adsorption and considers the existence of heterogeneous pore distribution [36]. The non-linear and linear form of this isotherm is expressed in Equations 18 and 19 respectively.

$$q_e = \left(\frac{A_{HJ}}{B_{HJ} - \log C_e}\right)^{\frac{1}{2}} \tag{18}$$

$$\frac{1}{q_e^2} = \frac{B_{HJ}}{A_{HJ}} - \left(\frac{1}{A_{HJ}}\right) log_{C_e} \tag{19}$$

In the above expressions, A_{HJ} denotes the multilayer adsorption while assuming the heterogeneous distribution of pores on the surface of TSB, and B_{HJ} indicate isotherm constant. These parameters were calculated from the slope and intercept of the Harkin

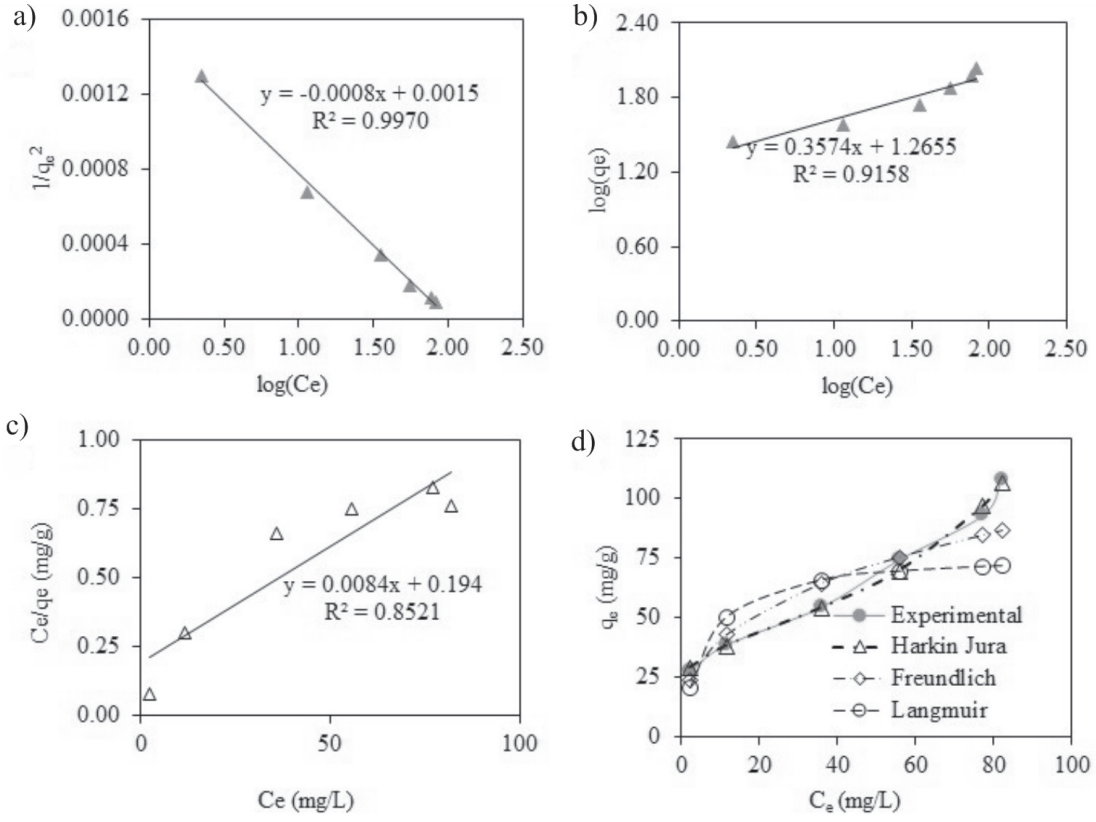

Fig. 4. Linear fit to RB5 adsorption by TSB a) = Harkin Jura, b) = Freundlich, c) = Langmuir, d) = deviation of RB5 adsorption capacity calculated by non-linear isotherm fitness from the experimental adsorption by TSB.

Jura plot $1/q_e^2$ versus $\log c_e$. Linear plot of Harkin-Jura's model is shown in Fig. 4. The values of A_{HJ} and B_{HJ} were calculated to be 1250 and 1.88 as well as 1414.41 and 2.04, respectively, in linear and non-linear regression analysis.

Freundlich isotherm [37] was used to further verify the nature of multilayer adsorption of RB5 as well as heterogeneity of the studied adsorbent. Non-linear (Equation 20) and linear (Equation 21) forms of this model are generally expressed as:

$$q_e = k_f c_e^{1/n} \quad (20)$$

$$\log q_e = \log(k_f) + \frac{1}{n}\log(c_e) \quad (21)$$

...where k_f is Freundlich constant, which is estimated adsorption capacity (mg/g) and n is the heterogeneity factor which demonstrate the favorability of the studied adsorption system. Adsorption process is considered linear if n = 1, physical (n>1) and chemical if n<0 [38]. The values of K_f and n were found to be 18.43 and 2.80, as well as 17.96 and 2.81, respectively, during linear and non-linear regression analysis. The values of *n* reveals the favorable physical adsorption of RB5 onto TSB adsorbent.

RB5 adsorption over the surface of TSB at 30ºC was also analyzed by non-linear (Equation 22) and and linear forms of Langmuir model (Equation 23). The latter assumes the monolayer adsorption and chemical interaction between adsorption site and RB5 dye molecules.

$$q_e = \frac{q_{e\,cal} K_L C_e}{1 + K_L C_e} \quad (22)$$

$$\frac{C_e}{q_e} = \frac{1}{K_L q_{e\,cal}} + \frac{C_e}{q_{e\,cal}} \quad (23)$$

...where K_L (L/mg) exhibits Langmuir constant. The values of $q_{e\,cal}$ (mg/g) and K_L (L/g) were found to be 119.05 and 0.043 as well as 76.99 and 0.163, respectively, in linear and non-linear regression. RB5 adsorption by TSB shows poor fit to Langmuir model with R^2 value of 0.8521 as shown in Fig. 4. This recommends that RB5 adsorptionn onto the TSB adsorbent followed multilayer phenomenon.

Error Analysis for Curve Fitting to Linear Isotherms

This is imperative to decide the best fit of equilibrium adsorption of RB5 by TSB biomass using error analysis approach for linear isotherms as inherent errors are introduced in linearization process. This also furnish a comparison of goodness of fit with non-linear isotherm. Table 1 describes the comparison of various errors analysed on fitting the linear isotherm. On the basis of R^2, isotherm fitness revealed the following order: Harkin-Jura (multilayer)>Freundlich (multilayer) >Langmuir (monolayer). Among the errors reported in current study, $\chi 2$ was found the best error method and precisely demonstrated the model parameter with lowest error value of 7.13 for Harkin-Jura.

Error Function Analysis for Curve Fitting to Non-Linear Isotherms

The coefficient of determination for isotherms and different error functions results from non-linear regression method are presented in Table 1. Non-linear isotherms revealed the better curve fitting which depict the smaller values of the error function. It was obvious that Harkin-Jura isotherm display a higher R^2 (closer to unity) and lower values of applied error functions compared to the rest of isotherm models. This suggests the Harkin-Jura is better than that of Freundlich and Langmuir isotherm models to represent equilibrium adsorption of RB5 dye onto TSB adsorbent.

Table 1. Error function analysis for isotherm fitness.

Error Functions	Linear			Non-linear		
	Harkin Jura	Freundlich	Langmuir	Harkin Jura	Freundlich	Langmuir
R^2	0.9970	0.9158	0.8521	0.9861	0.9469	0.9019
χ^2	7.13	7.60	20.26	0.04	6.8	19.45
ARE	13.16	12.73	21.17	1.1	12.19	20.19
S_{RE}	27.39	16.61	26.30	0.74	6.8	13.37
NSD	20.95	108.60	32.78	1.86	15.12	27.44
RMSE	18.20	85.90	15.43	0.91	9.87	14.46
MPSD	25.66	17.28	36.65	2.28	16.91	30.68
EABS	34.03	48.67	62.61	1.79	46.77	59.95
HYBRID	463.69	190.10	506.57	2.03	170.91	486.36
SSE	662.52	582.08	952.13	1.66	389.95	13.37

Table 2. Linear kinetic models parameters for RB5 adsorption onto TSB adsorbent.

Models	Parameters	Initial concentration of RB5 (mg/L)		
		20	40	80
	$q_{e\,exp}$ (mg/g)	18.06	29.85	47.20
PSO	$q_{e,\,cal}$ (mg/g)	19.19	29.94	49.02
	K_2 (1/min)	0.004	0.003	0.002
	R^2	0.9916	0.9899	0.9872
IPD	K_{pi} (mg/g $min^{1/2}$)	0.123	0.197	0.248
	Ci (mg/g)	11.25	17.83	32.08
	R^2	0.8927	0.9872	0.9908

This is also evident from the lower values of χ^2 that Chi-square error better describe the Harking-Jura isotherm non-linear fit as observed in case of linear regression fit to equilibrium data of the same model. Therefore, this confirms, from linear and non-linear regression analyses of isotherms fit, the formation of multilayer coverage of RB5 dye molecules at the external surface of the TSB surface.

Linear and Non-Linear Kinetic Models Curve Fitting and Error Function Analysis

The adsorption kinetics modelling explains the rate of adsorption of adsorbate from liquid to solid phase. RB5 dynamical adsorption data was fitted into linear and non-linear equations of pseudo-second order (PSO) (Equations 24 and 25) and intra-particle diffusion (IPD) (Equation 26) models. The possible adrsorption process for RB5 once in contact with TSB adsorbent in solution: (i) movement of RB5 molecules from bulk solution to the external boudary film adjascent to TSB adsorbent; attachment of dye molecules to the binding sites of TSB which is a rapid step and may include the physical adsorption or chemical (whether weak or strong) and/or both; (iii) RB5 diffusivity into the inner sites of TSB.

$$q_t = \frac{K_2 q_e^2\, t}{\left(1+\frac{1}{K_2 q_e t}\right)} \tag{24}$$

$$\frac{t}{q_t} = \frac{1}{K_2 q_e^2} + \frac{1}{q_e} t \tag{25}$$

$$q_t = K_{pi} t^{\frac{1}{2}} + C_i \tag{26}$$

The calculated values of kinetic model parameters, constants and R^2 are listed in Table 2. The comparative analysis of R^2 reflect higher googdness of RB5 data to to IPD kinetic compared to PSO with the increasing initial concentration of RB5 in the solution. Although R^2 value (0.9926) of PSO model fitness is observed high at low concentration of RB5, i.e., 20 mg/L, but the value of χ^2 error was found to be high, i.e., 0.25 than that of 0.11 for IPD model. RB5 data is fitted to IPD rather than PSO at 20 mg/L of RB5 dye. This suggest that the decreasing trend of PSO model fitness to RB5 is obvious from Table 2 and it can be seen that χ^2 error values increased from 0.25 to 1.13 with the increasing solution concentration and overall all the calculated errors were observed to be high for PSO model fitness than that calculated for IPD model. These observations validate that RB5 adsorption onto TSB is well described by IPD model than PSO model. The decreasing value of k_2 with increasing initial RB5 dye concentration (Table 2) reveals that sorbent sites may be diminished for higher concentration of RB5 molecules in the solution phase and there is possiblity of involvement of diffusion of RB5 molecules. The latter argument seems true because of increasing trend of K_{pi} and parametric boudary constant (C_i) values for IPD model.

In addition, the C_i for the IPD model from 11.55 to 32.08 also indicate pore filling mechanism and intraparticle diffusion of RB5 dye on the TSB surface [39]. However, all the linear plots were not passed through the origin, confirming that IPD mechanism was responsible for dye adsorption onto the surface of TSB but could not be designated as a sole rate limiting for the overall adsorption process and there may also be involvement of weak chemical interaction between RB5 and TSB surface as was noticed in FTIR study which reveal low chemical interaction.

In non-linear regression fit, the values of χ^2 error were found to be minimum among all the tested error functions for kinetic models (Table 3). Moreover, χ^2 error values for IPD model were smaller for IPD model than that of PSO which also reveals the kinetics of RB5 dye is better controlled by intra-particle diffusion phenomenon.

Regeneration of Spent TSB

The sustainability aspect of adsorbent is closely associated with the regeneration of adsorbent. It is clearly shown in Fig. 5 that mild hot water (50ºC) showed the maximum desorption efficiency for TSB adsorbent, i.e., 71%. Desorption efficiency for RB5-TSB

Table 3. Error functions for non-linear regression of RB5 adsorption to kinetic models.

Models	PSO kinetic model			IPD kinetic model		
Ci (mg/g) / Error function	20	40	80	20	40	80
R^2	0.9164	0.7983	0.7748	0.9461	0.9683	0.9774
χ^2	0.25	1.10	1.13	0.11	0.15	0.12
HYBRID	4.18	18.34	18.87	1.82	2.45	2.03
ARE	3.27	6.56	4.51	2.23	2.26	1.49
SRE	2.25	6.38	8.99	1.69	2.57	3.00
NSD	4.95	7.89	6.25	3.26	2.88	2.04
RMSE	0.96	2.62	3.42	0.63	0.96	1.12
MPSD	5.35	8.52	6.75	3.52	3.11	2.21
EABS	82.54	141.27	163.68	66.49	88.45	90.26
SSE	3.67	27.56	46.78	1.59	3.69	5.05

system was exhibited as DW-50ºC>DW-40ºC>NaOH (1 M)>NaOH (0.75 M)>NaOH (0.50 M)>NaOH (0.25 M). Maximum regeneration with DW-50ºC confirm the physical adsorption process followed during RB5 adsorption onto TSB. The application of mild hot water, as an effective eluent, was found more appropriate in terms environmental considerations.

Economic Analysis

The adsorbent and eluent costs are two major aspects which contribute to the sustainability of adsorption technique. The expenses involved in the collection, downsizing/grinding, washing and oven-drying of precursor materials were considered as stated elsewhere during cost analysis [40, 41]. The approximate cost involved in preparing 1 kg of TSB at laboratory scale was calculated in Pakistani rupees (PKR) and discussed below.

i. Cost of raw adsorbent (TSB)
purchased from local farmers in district Mansehra, KP, Pakistan = 3.0
ii. Transportation = 2.50
iii. Size-reduction and grindings cost
Hours × units × per unit cost = 0.05 × 0.4 × 5.79* = 0.12
iv. Washing of adsorbent 5 Liters × 10 = 50.0
v. Oven-drying Hours × units × per unit cost = 2.0 × 0.4 × 5.79* = 4.63
vi. Overhead budget (10%) = 6.25
vii. Total cost (per kg in PKR) = 66.50

As TSB adsorbent is readily available at minute cost, but transportation, preparation and energy (drying, grinding, sieving) and water would cost $0.40 per kg. Hence, TSB adsorbent may have an economic

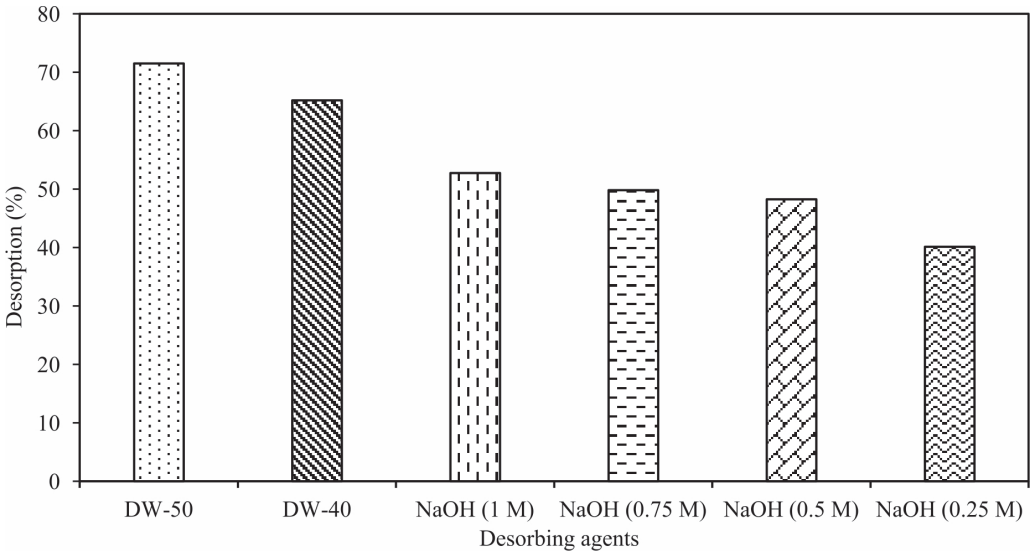

Fig. 5. Desorption and regeneration of spent TSB, DW (Distilled Water at 50ºC and 40ºC).

advantage over commercial adsorbents, particularly in developing world scenarios like Pakistan, to be used for the treatment of dye-loaded wastewater.

Conclusions

TSB is mostly disposed and an abundantly available agricultural waste material in Pakistan. TSB was successfully used for removal of RB5 dye from aqueous solution with maximum adsorption capacity of 92. 84 mg/g. The maximum RB5 removal efficiency for both reactive dyes were obtained at pH 2.0. Equilibrium data was fitted to linear and non-linear isotherms and kinetic models. RB5 adsorption onto TSB followed multilayer, data displayed good fit to Harkin-Jura high R^2 (R^2 = 0.9970 for linear and 0.9861 for non-linear) followed by Freundlich model with R^2 of 0.9158 for linear and 0.9469 for non-linear with R^2. SEM and FTIR analyses exhibited visible macroporous structures and low chemical interaction respectively. RB5 kinetic was found best explained by intraparticle diffusion model at increasing concentration of dye in the solution. Likewise error analysis for all the tested error functions exhibited lower errors for intraparticle diffusion model than that of PSO model which reinforce the better dynamical description of RB5 over the surface of TSB with IPD model. In linear and non-linear regression fit, the values of χ^2 error were found to be minimum among all the tested error functions and; therefore this error method is found best to explain the isotherm and kinetic models fitness. Thermodynamics parameters unfolded the spontaneous and enothermic nature of RB5 adsorption onto TSB adsorbent. Distilled mild hot water was found as suitable desorbing elluent which also support the multilayer adsorption process in the investigated RB5-TSB system. This study also recommended that the TSB could be considered as an effective and economically viable waste for the removal of RB5.

Acknowledgements

This research has been funded by Research Deanship of University of Ha'il - Saudi Arabia through project number RG-191313

Conflicts of Interest

The authors declare no conflict of interest.

References

1. AREVALO-GALLEGOS A., AHMAD Z., ASGHER M., PARRA-SALDIVAR R., IQBAL H.M.N. Lignocellulose: A sustainable material to produce value-added products with a zero waste approach – A review, Int. J. Biol. Macromol. **99**, 308, **2017**.
2. EZER G.G., ARıCı M., ERUCAR İ., YEŞILEL O.Z., ÖZEL H.U., GEMICI B.T., ERER H. Zinc (II) and cadmium (II) coordination polymers containing phenylenediacetate and 4,4′-azobis(pyridine) ligands: Syntheses, structures, dye adsorption properties and molecular dynamics simulations, J. Solid Stat. Chem. **255**, 89, **2017**.
3. ROBINSON T., MCMULLAN G., MARCHANT R., NIGAM P. Remediation of dyes in textile effluent: a critical review on current treatment technologies with a proposed alternative, Bioresour. Technol. **77**, 247, **2001**.
4. EL BOURAIE M., EL DIN W.S. Biodegradation of reactive black 5 by *Aeromonas hydrophila* strain isolated from dye-contaminated textile wastewater, Sustain. Environ. Res. **26**, 209, **2016**.
5. SUN B., YUAN Y., LI H., LI X., ZHANG C., GUO F., LIU X., WANG K., ZHAO X.S. Waste-cellulose-derived porous carbon adsorbents for methyl orange removal, Chem. Eng. J. **371**, 55, **2019**.
6. OGUNTIMEIN G.B. Biosorption of dye from textile wastewater effluent onto alkali treated dried sunflower seed hull and design of a batch adsorber, J. Environ. Chem. Eng. **3**, 2647, **2015**.
7. DEGERMENCI G.D., DEGERMENCI N., AYVAOGLU V., DURMAZ E., CAKıR D., AKAN E. Adsorption of reactive dyes on lignocellulosic waste; characterization, equilibrium, kinetic and thermodynamic studies, J. Clean. Prod. **225**, 1220, **2019**.
8. HUSSAIN GARDAZI S.M., ASHFAQ BUTT T., RASHID N., PERVEZ A., MAHMOOD Q., MAROOF SHAH M., BILAL M. Effective adsorption of cationic dye from aqueous solution using low-cost corncob in batch and column studies, Desalin. Water Treat. **57**, 28981, **2016**.
9. CICEK F., OZER D., OZER A., OZER A. Low cost removal of reactive dyes using wheat bran, J. Hazard. Mater. **146**, 408, **2007**.
10. DENIZ F. Dye removal by almond shell residues: Studies on biosorption performance and process design, Mater. Sci. Eng. : C. **33**, 2821, **2013**.
11. TRAN H.N., YOU S.-J., NGUYEN T.V., CHAO H.-P. Insight into the adsorption mechanism of cationic dye onto biosorbents derived from agricultural wastes, Chem. Eng. Commun. **204**, 1020, **2017**.
12. AHMED M.J. Preparation of activated carbons from date (*Phoenix dactylifera* L.) palm stones and application for wastewater treatments: Review, Process Saf Environ Prot. **102**, 168, **2016**.
13. REHMAN S., ADIL A., SHAIKH A.J., SHAH J.A., ARSHAD M., ALI M.A., BILAL M. Role of sorption energy and chemisorption in batch methylene blue and Cu^{2+} adsorption by novel thuja cone carbon in binary component system: linear and nonlinear modeling, Environ. Sci. Pollut. Res. **25**, 31579, **2018**.
14. KARRI R.R., SAHU J., JAYAKUMAR N. Optimal isotherm parameters for phenol adsorption from aqueous solutions onto coconut shell based activated carbon: error analysis of linear and non-linear methods, J. Taiwan Inst. Chem. E. **80**, 472, **2017**.
15. PRASAD A.L., SANTHI T., MANONMANI S. Recent developments in preparation of activated carbons by microwave: Study of residual errors, Arab. J. Chem. **8**, 343, **2015**.
16. POPOOLA L.T. Characterization and adsorptive behaviour of snail shell-rice husk (SS-RH) calcined particles (CPs) towards cationic dye, Heliyon. **5**, e01153, **2019**.

17. MIRABOUTALEBI S.M., NIKOUZAD S.K., PEYDAYESH M., ALLAHGHOLI N., VAFAJOO L., MCKAY G. Methylene blue adsorption via maize silk powder: kinetic, equilibrium, thermodynamic studies and residual error analysis, Process Saf. Environ. **106**, 191, **2017**.
18. KAM W., LIEW C.-W., LIM J.Y., RAMESH S. Electrical, structural, and thermal studies of antimony trioxide-doped poly(acrylic acid)-based composite polymer electrolytes, Ionics. **20**, 665, **2014**.
19. JESURANI S., KANAGESAN S., VELMURUGAN R., KALAIVANI T. Phase formation and high dielectric constant of calcium copper titanate using sol-gel route, J. Mater. Sci-Mater. **23**, 668, **2012**.
20. BODIRLAU R., TEACA C. Fourier transform infrared spectroscopy and thermal analysis of lignocellulose fillers treated with organic anhydrides, Rom. J. Phys. **54**, 93, **2009**.
21. KANAGATHARA N., SHENBAGARAJAN P., JEYANTHI C.E., THIRUNAVUKKARASU M. Fourier transform infrared spectroscopic investigation on Nifidipine, Int. J. Pharm. Biol. Sci. **1**, 52, **2011**.
22. SAIKIA B.J., PARTHASARATHY G. Fourier transform infrared spectroscopic characterization of kaolinite from Assam and Meghalaya, Northeastern India, J. Mod. Phys. **1**, 206, **2010**.
23. TUNC O., TANACI H., AKSU Z. Potential use of cotton plant wastes for the removal of remazol black B reactive dye, J. Hazard. Mater. **163**, 187, **2009**.
24. SUN D., ZHANG X., WU Y., LIU X. Adsorption of anionic dyes from aqueous solution on fly ash, J. Hazard. Mater. **181**, 335, **2010**.
25. MAURER H.W. Chapter 18 - Starch in the Paper Industry, in: J. BeMiller, R. Whistler (Eds.) Starch (Third Edition), Academic Press, San Diego, 657, **2009**.
26. HONORIO J.F., VEIT M.T., GONCALVES G.D.C., DE CAMPOS E.A., FAGUNDES-KLEN M.R. Adsorption of reactive blue BF-5G dye by soybean hulls: kinetics, equilibrium and influencing factors, Water Sci. Technol. **73**, 1166, **2015**.
27. GAO J., SI C., HE Y. Application of soybean residue (okara) as a low-cost adsorbent for reactive dye removal from aqueous solution, Desalin. Water Treat. **53**, 2266, **2015**.
28. FETTOUCHE S., TAHIRI M., MADHOUNI R., CHERKAOUI O. Removal of reactive dyes from aqueous solution by adsorption onto alfa fibers powder, J. Mater. Environ. Sci. **6**, 129, **2015**.
29. MORAIS L., FREITAS O., GONCALVES E., VASCONCELOS L., BECA C.G. Reactive dyes removal from wastewaters by adsorption on eucalyptus bark: variables that define the process, Water Res. Ind. **33**, 979, **1999**.
30. SAEED M., NADEEM R., YOUSAF M. Removal of industrial pollutant (reactive orange 122 dye) using environment-friendly sorbent *Trapa bispinosa*'s peel and fruit, Int. . Eiron. Sci. Technol. **12**, 1223, **2015**.
31. KRAGOVIC M.M., STOJMENOVIC M., PETROVIC J.T., LOREDO J., PASALIC S., NEDELJKOVIC A., RISTOVIC I. Influence of alginate encapsulation on point of zero charge (pHpzc) and thermodynamic properties of the natural and Fe (III)-modified zeolite, Procedia Manuf. **32**, 286, **2019**.
32. MASHKOOR F., NASAR A. Preparation, characterization and adsorption studies of the chemically modified *Luffa aegyptica* peel as a potential adsorbent for the removal of malachite green from aqueous solution, J. Mol. Liq. **274**, 315, **2019**.
33. DURAL M.U., CAVAS L., PAPAGEORGIOU S.K., KATSAROS F.K. Methylene blue adsorption on activated carbon prepared from *Posidonia oceanica* (L.) dead leaves: Kinetics and equilibrium studies, Chem. Eng. J. **168**, 77, **2011**.
34. INYINBOR A., ADEKOLA F., OLATUNJI G.A. Kinetics, isotherms and thermodynamic modeling of liquid phase adsorption of Rhodamine B dye onto *Raphia hookerie* fruit epicarp, Water Res. Ind. **15**, 14, **2016**.
35. KHAN M.M.R., SAHOO B., MUKHERJEE A.K., NASKAR A. Biosorption of acid yellow-99 using mango (*Mangifera indica*) leaf powder, an economic agricultural waste, SN Appl. Sci. **1**, 1493, **2019**
36. HARKINS W.D., JURA G. Surfaces of solids. XIII. A vapor adsorption method for the determination of the area of a solid without the assumption of a molecular area, and the areas occupied by nitrogen and other molecules on the surface of a solid, J. Am. Chem. Soc. **66**, 1366, **1944**.
37. FREUNDLICH H. Over the adsorption in solution, J. Phys. Chem. **57**, 1100, **1906**.
38. ZAHEER Z., BAWAZIR W.A., AL-BUKHARI S.M., BASALEH A.S. Adsorption, equilibrium isotherm, and thermodynamic studies to the removal of acid orange 7, Mater. Chem. Phys. **232**, 109, **2019**.
39. REHMAN S., TARIQ M., SHAH J.A., AHMAD R., SHAHZAD M., ABBASI A.M., ULLAH A., ISMAIL B., BILAL M. Simultaneous physisorption and chemisorption of reactive Orange 16 onto hemp stalks activated carbon: proof from isotherm modeling, Biointerface Res. Appl. Chem. **7**, 2021, **2017**.
40. SHAH J.A., BUTT T.A., MIRZA C.R., SHAIKH A.J., KHAN M.S., ARSHAD M., RIAZ N., HAROON H., GARDAZI S.M.H., YAQOOB K. Phosphoric acid activated carbon from *Melia azedarach* waste sawdust for adsorptive removal of reactive orange 16: Equilibrium modelling and thermodynamic analysis, Molecules. **25**, 2118, **2020**.
41. DHAWANE S.H., KUMAR T., HALDER G. Biodiesel synthesis from *Hevea brasiliensis* oil employing carbon supported heterogeneous catalyst: Optimization by Taguchi method, Renew. Energy. **89**, 506, **2016**.